

Perceptual Quality Assessment of Face Video Compression: A Benchmark and An Effective Method

Yixuan Li, Bolin Chen, Baoliang Chen, Meng Wang, and Shiqi Wang, *Senior Member, IEEE*

Abstract

Recent years have witnessed an exponential increase in the demand for face video compression, and the success of artificial intelligence has expanded the boundaries beyond traditional hybrid video coding. Generative coding approaches have been identified as promising alternatives with reasonable perceptual rate-distortion trade-offs, leveraging the statistical priors of face videos. However, the great diversity of distortion types in spatial and temporal domains, ranging from the traditional hybrid coding frameworks to generative models, present grand challenges in compressed face video quality assessment (VQA) that plays a crucial role in the whole delivery chain for quality monitoring and optimization. In this paper, we introduce the large-scale Compressed Face Video Quality Assessment (CFVQA) database, which is the first attempt to systematically understand the perceptual quality and diversified compression distortions in face videos. The database contains 3,240 compressed face video clips in multiple compression levels, which are derived from 135 source videos with diversified content using six representative video codecs, including two traditional methods based on hybrid coding frameworks, two end-to-end methods, and two generative methods. The unique characteristics of CFVQA, including large-scale, fine-grained, great content diversity, and cross-compression distortion types, make the benchmarking for existing image quality assessment (IQA) and VQA feasible and practical. The results reveal the weakness of existing IQA and VQA models, posing challenges on real-world face video applications. In addition, a Face Video Integrity (FAVOR) index for face video compression was developed to measure the perceptual quality, considering the distinct content characteristics and temporal priors of the face videos. Experimental results exhibit its superior performance on the proposed CFVQA dataset. The benchmark is now made publicly available at: <https://github.com/Yixuan423/Compressed-Face-Videos-Quality-Assessment>.

Index Terms

Face video compression, video quality assessment, subjective and objective study.

I. INTRODUCTION

FACE video based services have been growing exponentially in the past decade, coinciding with the accelerated proliferation of mobile devices and online video content sharing platforms. Face video compression, which is indispensable in compressing and delivering gigantic-scale face video data, introduces inevitable distortions, degrading the perceptual video quality. Therefore, it is of prominent importance to study the quality assessment of compressed face videos, which is recognized as an essential component in warranting the modern services for face video compression, transmission, and storage systems.

Over the years, advancements in video compression technology have quintessentially benefited face video compression. Dating back to the 1970s, Netravali and Stuller [1] pioneered to propose a block-based motion compensation transform framework, which became the cornerstone of the hybrid prediction schemes broadly employed nowadays. Since the 2000s, video coding standards such as H.264/Advanced Video Coding (AVC) [2], H.265/High Efficiency Video Coding (HEVC) [3], and H.266/Versatile Video Coding (VVC) [4] have been developed and widely adopted for both academic and commercial applications. Recently, deep learning has boosted numerous data-driven algorithms [5]–[10], in particular the end-to-end (E2E) schemes that jointly optimize the compression process as a whole. For example, Lu *et al.* [5] proposed the first E2E deep video compression framework (DVC) for competitive rate-distortion (RD) performance. Similarly, Yang *et al.* [6] proposed a Recurrent Learned Video Compression (RLVC) framework to leverage temporal correlation among video frames and improve the RD performance. The statistical regularities which serve as the solid facial priors have motivated a series of face video compression algorithms. The pioneering compression scheme dedicated to the human face was proposed in [11], where the 3D head model was adopted. The deep generative models such as variational auto-encoding (VAE) and generative adversarial networks (GANs) have also been leveraged in face video compression. In particular, Wiles *et al.* [12] proposed the X2Face to generate human faces using audio and pose code, which can be further applied to face compression. The ultra-low bit-rate few-shot video-to-video synthesis [13] scheme was proposed in 2019, which translates raw videos to the compact version via the key-point representations. The First Order Motion Model (FOMM) [14] was proposed for face image animation, based on which Oquab *et al.* proposed [15] for mobile video chat scenarios. Moreover, Chen *et al.* [16] proposed an E2E talking-head video compression framework (CFTE) via compact feature learning, achieving high compression efficiency under ultra-low bit rate scenarios. These face-specific video coding methods targeting low bit-rate have been claimed to be efficient in providing much better visual quality at the same level of coding bits.

Though numerous codecs have been proposed for face video compression, there is no universal one that could achieve the ever-best performance in all application scenarios to our knowledge. Therefore, there have been great concerns about how

the quality varies throughout the video production and delivery chain for different compression methods and how the whole system could be optimized with immediate resource allocation. While existing video quality assessment (VQA) measures can be adopted for compressed face video quality assessment, there are fundamental limits. On the one hand, face quality assessment is essentially at the cognitive level due to the distinct preference for a “good-looking” face. One typical example is that HVS prefers the appropriate level of face smoothness instead of contrast enhancement. Moreover, prominent factors such as symmetry and realness of the human face’s geometric priors can also dominate face quality. On the other hand, homogeneous face areas that cannot potentially mask high-contrast distortions are sensitive to induced compression noise. Considering the compression artifacts from different codecs, including both traditional artifacts and the artifacts generated by the CNNs and GANs, the quality measure that achieves reliable cross-distortion face quality prediction is highly demanded.

However, the research on perceptual face video quality assessment has primarily escaped the research attention, including both subjective studies and objective measures. Herein, we conduct a comprehensive and systematic study on the perceptual quality of compressed face videos. Specifically, we establish the first large-scale, fine-grained subjective quality benchmark for compressed face videos, conduct thorough subjective opinions analyses, and propose a dedicated full-reference (FR) objective quality evaluation framework for compressed face videos. The proposed benchmark and quality measure are also expected to shed light on developing the next-generation face compression algorithms. In summary, the contributions of this paper are as follows,

- We build the first-of-a-kind perceptual video quality assessment benchmark for face video compression. There are several unique characteristics for the proposed Compressed Face Video Quality Assessment (CFVQA) dataset, including diverse video content spanning a wide range of real-world scenarios, different compression methods such as conventional hybrid coding, E2E coding, and GAN-based coding dedicated to face videos, and rigorous subjective testing with statistical processing.
- We analyze the perceptual distortions in compressed face videos from the perspective of distortion type, level and perceptual RD performance. We also qualitatively compare Human Visual System’s (HVS) sensitivity to different compression distortions. We demonstrate the weakness of the top-performance FR models, and careful explorations of these models provide the insights into the potential ways for future improvement.
- We propose a new FR perceptual quality assessment method dedicated for compressed face videos, taking human face priors and quality perception characteristics in the temporal domain into consideration. The method achieves superior performance on the proposed database compared with other popular quality assessment methods. This study points a new avenue for the future face quality assessment research.

II. RELATED WORK

A. Quality Assessment of General-content Videos

1) *Subjective Video Quality Assessment*: Subjective quality assessment is the most reliable and straightforward way to evaluate visual quality. In particular, the subjective video quality assessment datasets, which contain distorted videos with diverse content, distortion types and levels, could serve as the golden ground truth in fairly comparing and testing the performance of different objective quality assessment models and shed light on the development of the next-generation VQA and video coding algorithms. Recently, several well-known datasets have been constructed for VQA, including authentic-distorted datasets and artificial-distorted datasets. In 2009, Simone *et al.* [23] proposed the first subjective VQA dataset targeting exploring the video quality degradation caused by transmission packet loss. Subsequently, several datasets [24]–[34] focusing on compressed video quality were proposed, which significantly boost the evolution of FR objective measures. Besides, the VQA datasets containing authentic distortions [17]–[22] also contribute significantly to the development of no-reference(NR) VQA methods. The summary of the aforementioned datasets can be found in Table I.

Although these datasets have significantly contributed to the development of the VQA research, there are some fundamental limitations for the particular task studied in this work. First, the content of the existing datasets is not restricted to an dedicated narrow scope solely with face videos that are deemed to have unique domain pattern. Second, the distortion types of existing datasets are conventional (e.g., H.264/AVC or H.265/HEVC compression), and the distortions generated by learning-based compression algorithms, including E2E codecs and generative compression schemes are not considered. Third, a large-scale dataset with diverse content is highly desired, while a typical issue of the existing datasets is the limited number of reference videos with human faces. To meet the enormous demand for benchmarking and developing face video compression methods, we propose a largest-of-its-kind dataset with 135 reference videos and 3,240 compressed videos from six different compression methods.

2) *Objective Video Quality Assessment*: The FR-VQA/IQA algorithms which quantify image quality by measuring the similarity between the reference and distorted videos, have been widely applied in video compression performance evaluation and optimization [5], [6], [16], [35]. The most popular method peak signal-to-noise ratio (PSNR) has been widely criticized due to the low correlation with the HVS [36]. The structural similarity index (SSIM) [37] and its variants [38]–[43] have been developed with the design philosophy that the HVS is excelling in extracting the structural information. Recently, deep-learning-based IQA methods like learned perceptual image patch similarity (LPIPS) [44] and deep image structure and texture

TABLE I
COMPARISON WITH THE PREVIOUS VQA DATASETS. THE NOTION “–” DENOTES THAT THE DATASET IS AN AUTHENTIC DISTORTED DATASET, AND CONTAINS NO REFERENCE VIDEOS BUT ONLY DISTORTED VIDEOS.

Dataset	#Reference videos	Video Content	#Distorted videos	#Distortion types	Distortion types
CVD2014 [17]	–	universal	234	–	authentic distortions
KoNViD-1k [18]	–	universal	1,200	–	authentic distortions
LIVE-Qualcomm [19]	–	UGC	208	–	authentic distortions
LIVE-VQC [20]	–	UGC	585	–	authentic distortions
Youtube-UGC [21]	–	UGC	1,500	–	authentic distortions
LSVQ [22]	–	UGC	38,811	–	authentic distortions
EPFL-PoliMI [23], [24]	12	universal	144	1	transmission packet loss
LIVE-Mobile [25]	10	universal	200	5	AVC SVC compression, transmission packet loss, frame-freeze, rate adaption, temporal dynamics
LIVE [26]	10	universal	150	4	MPEG-2 and AVC compression, transmission packet loss in two modes
IVP [27]	10	universal	128	4	Dirac wavelet compression, AVC compression, transmission packet loss, MPEG-2 compression
IVC-IC [28]	60	universal	240	1	AVC SVC compression
TUM-HD [29]	8	universal	32	1	MPEG compression
MCL-JCV [30], [31]	220	universal	45,760	1	H.264 compression
MCML-4K [32]	10	universal	240	3	AVC, HEVC, and VP9 compression
LIVE-Netflix [33]	14	universal	112	3	re-buffering events, dynamically changing AVC compression rates, mixture of both
BVI-HD [34]	32	universal	384	1	HEVC compression
CFVQA (OURS)	135	human face	3,240	6	VVC compression, reduced resolution compression, two E2E compression algorithms, two generative compression algorithms

similarity (DISTS) [45] quantify the similarity in the deep-feature domain. In [46], the reference and distorted features are compared with the Wasserstein distance. In [47], it shows that DISTS and LPIPS deliver average-level yet the best performance on generative image compression among all IQA methods. Though the prediction accuracy is unsatisfactory, the two measures are still used to evaluate the performance of generative face video compression [16] because of the computational efficiency.

Video quality assessment involves the temporal domain which significantly influences perceptual quality. To measure quality degradation in the temporal domain, a series of non-blind VQA approaches [48]–[55] perform satisfactorily on the general-content video quality assessment task. For instance, in [49], the authors developed the motion-based video integrity evaluation (MOVIE) based on the spatial frequency and orientation selectivity of the HVS. In [50], Moorthy *et al.* proposed a motion-compensated structural similarity index (MC-SSIM) that balances the trade-off between motion information and computational cost. In 2016, the video multimethod assessment fusion model (VMAF) [52] was proposed and became a popular performance evaluation criterion for video codecs. Besides, reduced-reference VQA methods [56], [57] also significantly contribute the quality evaluation of compressed videos. Although these VQA models achieve good correlations with the HVS, they are not specifically designed for face videos, leading to less satisfactory performance. Such conflict leads us to rethink the effective and efficient perceptual quality evaluation methods for compressed face videos.

B. Quality Assessment of Face Videos

The face image/video quality assessment (FIQA/FVQA) is a long-standing research problem, typically referring to two research areas. The most-developed one is sourced from the biometrics community, targeting at investigating the recognizability of face images or videos as the input to face recognition systems. The pioneering work of this kind was proposed in [58], where face asymmetries due to lighting and face pose are quantified. Subsequently, numerous FIQA algorithms emerge by extracting quality-aware features in a handcrafted [59]–[62] or learning way [63]–[67]. For instance, Zhang *et al.* [68] propose a illumination quality dataset of face images and a deep-learning-based measure. Terhorst *et al.* [66] proposed the SER-FIQ which computes the Euclidean distance of the unsupervised quality-aware features as face quality measure. In 2021, Schlett *et al.* [69] provide a comprehensive survey on biometric FIQA, summarizing representative FIQA databases and methodologies. However, these methods are not dedicated to compressed face videos, although certain connections could exist. Due to the

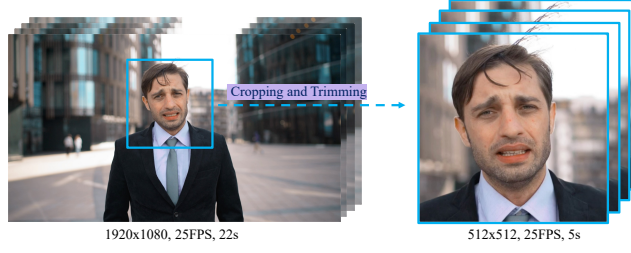


Fig. 1. Illustration of the pre-processing for the reference video sequences.

distinction of the ultimate receiver, biometric evaluation methods cannot be directly utilized for evaluating the perceptual quality of compressed face videos.

In contrast, another research line is assessing the perceptual quality of face images/videos in terms of Quality of Experience (QoE). In [70], Su *et al.* created the first IQA database of in-the-wild human faces called GFIQA-20k and proposed a blind FIQA model based on the generative face prior. In [71], Jo *et al.* proposed another blind FIQA method assessing the perceptual realness of face images. However, both subjective and objective quality assessment for compressed face videos is still out of the research attention. Our elaborately designed dataset and the proposed model could mitigate such the gap and shed the light on high-quality face video compression.

III. CONSTRUCTING THE CFVQA DATASET

A. Face Video Content



Fig. 2. Sample frames from reference videos in this benchmark. In total, there are 135 different reference face videos in the CFVQA, covering a great range of content diversity.

We construct the CFVQA dataset including 135 reference and 3,240 distorted face videos spanning a considerable diversity of face video content, in terms of various ages, ethnicity, appearances, expressions, head positions, head motion trails, camera motions, backgrounds, etc. The CFVQA also has good accessories coverage, like glasses, headsets, hijab, hairbands, etc. To this end, we have carefully collected source videos according to the following principles,

- With the resolution higher than 1080×960 ($w \times h$);
- With the frame rate of 25 frames per second (FPS);
- Containing unobstructed human face;
- Lasting longer than 5 seconds;

- No visually distinguishable artifacts based on sophisticated manual examination.

The source face videos are obtained from two copyright-free websites, Pexels.com [72] and Mixkit.com [73], where the videos are permitted to use, modified, and redistributed freely without attribution. As shown in Fig. 1, considering the application scenarios, we crop the 512×512 patch containing the face from the original video sequence, where the face area takes no less than one quarter of the entire patch size. As suggested in [74], [75], sequences of five seconds are truncated from each raw video, leading to 135 face videos with 16,875 frames, which are in the resolution of 512×512 , during for 5 seconds, and frame rate at 25 fps. In Fig. 2, sample frames of reference face videos are illustrated.

B. Face Video Compression

There are six video compression methods employed to generate compressed videos in the proposed benchmark. The details of the video codecs are as follows,

- VVC [4]: Relying on the block-based hybrid coding framework.
- Reduced resolution (RL): Following the *Downsampling, VVC compression and Upsampling* workflow. The bicubic downsampling and upsampling are adopted.
- DVC [5]: End-to-end framework with learning-based optical flow motion estimation module and auto-encoder style compression module.
- RLVC [6]: End-to-end framework with recurrent auto-encoder and recurrent probability model.
- FOMM [14]: GAN-based model with keypoint representation.
- CFTE [16]: GAN-based model with deep learning based feature representation.

Each reference video is compressed by these codecs to three to five compression levels. Regarding the selection of the compression parameters (i.e., quantization parameters, QP), we follow two principles. First, the separation of different levels by adjusting the QPs enables a wide range of quality levels covered. Second, we ensure the alignment of the quality level for different compression methods by a small-scale subjective study that are detailed in supplementary. The final selected QPs for each codec are listed in Table II. In total, $135 \times 24 = 3,240$ compressed face videos are generated from 135 reference face videos.

TABLE II
SELECTED QP VALUES FOR EACH COMPRESSION METHOD IN THIS BENCHMARK

Method	QP	Number
VVC	22, 32, 37, 42, 47	675
RL	32 with down-sample ratios 0.25, 0.5, 0.75	405
DVC	22, 32, 37, 42	540
RLVC	22, 27, 32, 37	540
FOMM	22, 32, 37, 42	540
CFTE	22, 32, 37, 42	540
Overall	–	3,240

Herein, we provide thorough analyses of compression distortions in our benchmark, and more details can be found in the supplementary.

1) Spatial-domain Artifacts:

- Blur. Blur has been the most commonly involved distortion type in modern video compression. In particular, blur manifests itself in diversified forms in all six video compression methods, potentially degrading information fidelity. However, in some occasions, blur does not necessarily degrade QoE of face videos, especially in the video collections by E2E compression methods, as evidenced by the user survey detailed in the supplementary [76].
- Blockiness. Blockiness has been the very typical compression distortion type in the VVC coding framework, resulting in visually disturbing discontinuities on the block boundaries. As such, blockiness artifacts have been observed to appear in the videos compressed by VVC and RL methods.
- Edge artifacts. In this study, edge artifact is designated as widened edges and fake edges, which is caused by up-sampling and down-sampling in the reduced resolution compression method. Such artifacts are perceived in all six video subsets, and the CFTE, FOMM and RL are the three most-seen subsets. For example, in Fig. 3, fake edges can be found near normal edges in the RL-compressed video frames caused by the upsampling.
- Geometric distortions. Geometric distortion is comprised of content twisting and shape change in this study, which originates from generative models. This kind of distortion is most eye-catching and annoying according to the user study in supplementary. Fig. 3 provides exemplar frames from CFTE and FOMM-compressed videos, where the face area is twisted weirdly, and some content is falsely eliminated. Such artifacts often cause the sense of unreality of human faces.

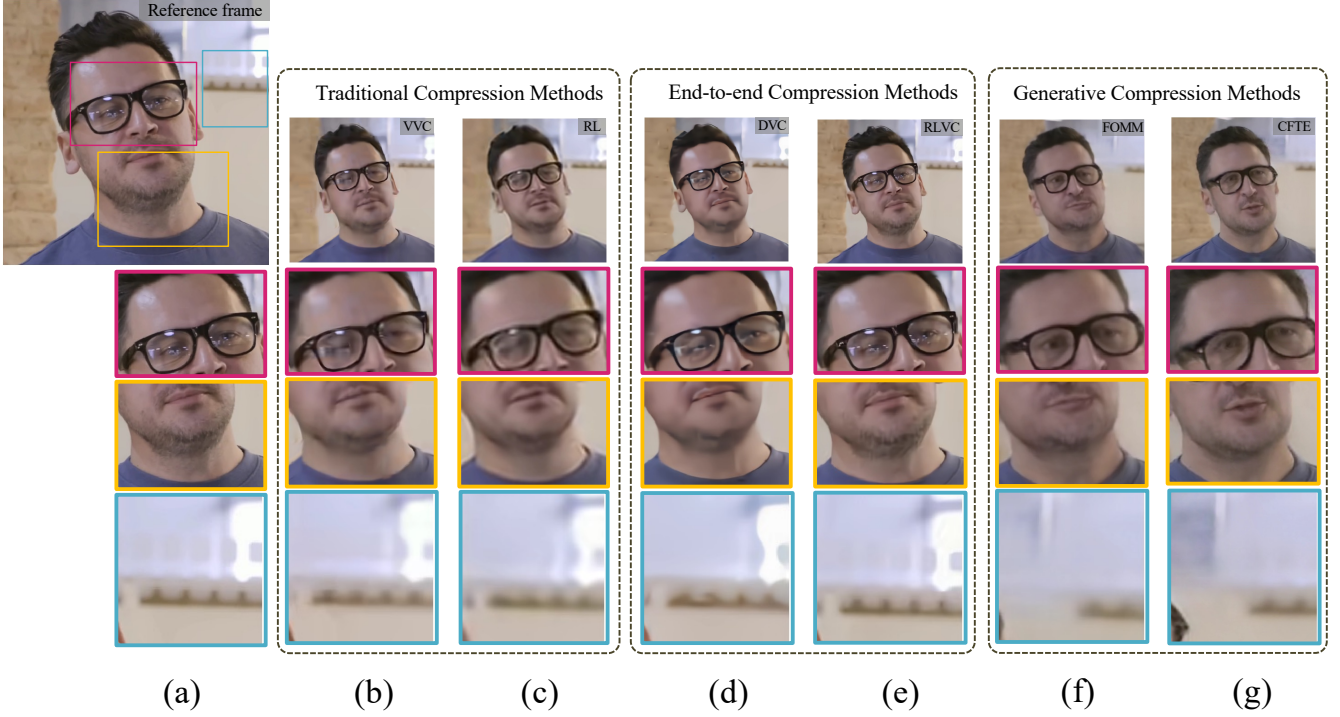


Fig. 3. Illustrations of the spatial distortions in compressed face videos. (a) Reference frame and corresponding patches from the CFVQA; (b) VVC; (c) RL; (d) DVC; (e) RLVC; (f) FOMM; (g) CFTE.



Fig. 4. Illustrations of the perceptual temporal distortions in compressed face videos. Three successive frames are utilized for reference and distortion comparisons. The images are better viewed with zooming.

2) Temporal-domain Artifacts:

- **Flickering.** Flickering artifact refers to frequent transients in terms of luminance, chrominance, and texture existing locally or globally in the video. In Fig. 5, we analyze the frame-level quality by computing the average DISTS value of a particular frame over all test video sequences. Apparently, the flickering artifact can be induced due to the quality punctuation caused by E2E compression models, finally bringing quality degradation. This phenomenon could be further verified by the user

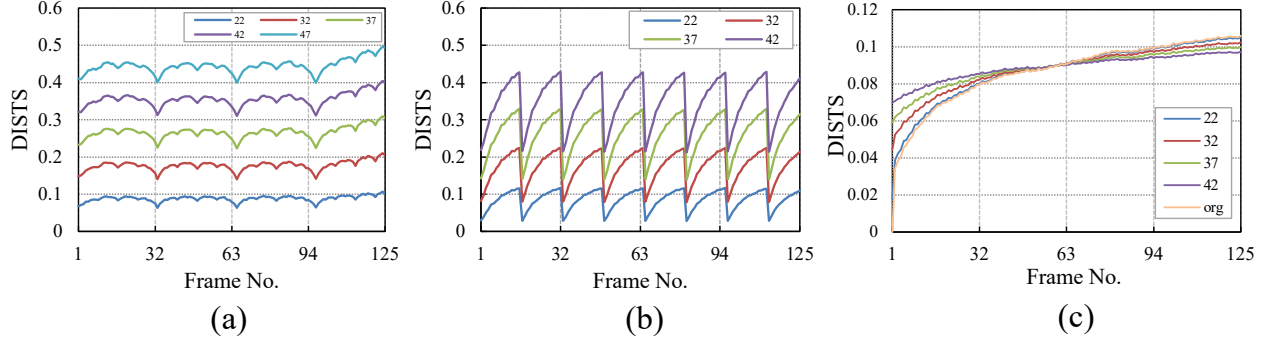


Fig. 5. Illustrations of frame-level quality fluctuations in terms of DISTs. (a) VVC compressed videos; (b) DVC-compressed videos; (c) FOMM-compressed videos. More specifically, in (c), the “org” data correspond to the videos compressed by FOMM with a pristine key frame.

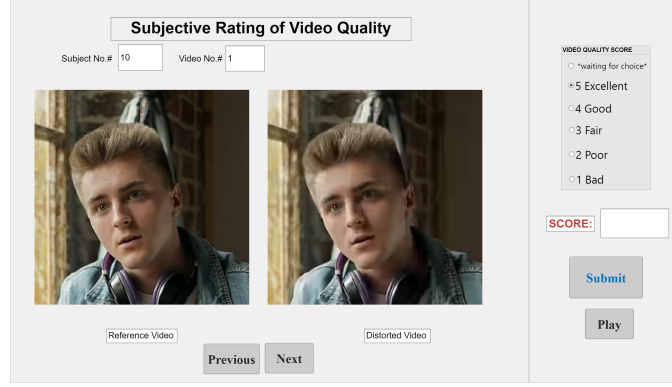


Fig. 6. Screenshot of the subjective testing interface.

study results in the supplementary. As shown in Fig. 4, the texture of three consecutive frames compressed by DVC and RLVC codecs shows apparent variations, and such inconsistency is visually perceived as the flashing effects in local regions.

- **Floating.** Floating artifact refers to the appearance of illusive motion in certain regions as opposed to their surrounding background [77]. Such artifacts often lead to abnormal jello-like content wobbling in the compressed face video. The face videos compressed by generative models typically show distinct floating artifacts manifested as two forms. On one hand, the stationary background areas surrounding face boundaries can even move along with the face. On the other hand, certain areas may not vary along with the global camera motion. As a result of erroneous motion estimation in generative coding methods, temporal floating always brings annoying visual perception artifacts.

C. Subjective Testing

Following ITU-R P.910 [78], the subjective quality evaluation protocol is designed with the set-up testing environment. We adopt the Double-Stimulus Continuous Quality Evaluation (DSCQE) [79] approach with the 5-category discrete Absolute Rating Scale (ARS) [80] in our test. Under double stimulus protocol, both the reference and distorted videos are displayed. The subjects shall score the distorted video by comparing the perceived quality difference between reference and distorted ones. The DSCQE is more robust to the variations of the video content by taking fidelity into consideration. More specifically, the reference and compressed videos are juxtaposed and displayed successively. Being aware of the reference videos, the subjects are required to rate the quality of the compressed face video after viewing the video pairs. The user interface used in our test is shown in Fig. 6. The reference and compressed face videos are loaded into the memory before each rating round to guarantee displaying fluency. The right side contains five labels for the users to rate quality adequately, including “Excellent”, “Good”, “Fair”, “Poor”, and “Bad” from the lowest level to the highest, denoting the quality scores ranging from 5 to 1. The 4K screen with the resolution of $3,840 \times 2,160$ in normal indoor lighting conditions is utilized. All the videos are displayed at their original resolution without zooming in or out to avoid any distortions caused by scaling.

Before the subjective test, a brief tutorial is conducted for education and guidance purposes. In the tutorial, exemplar cases of common video distortion types at severity levels as well as factors concerning quality rating (e.g., perceived quality and information fidelity), are shown. Moreover, it is also clearly stated that the influence of facial aesthetics is attempted to be minimized in the test. In order to reduce the effect of viewer fatigue, the 3,240 compressed face videos are divided into 13

individual sessions, each lasting no longer than one hour. The time interval between sessions is at least 24 hours. Moreover, to further avoid memory and contextual effect, the compressed videos in each session are randomly selected and thoroughly shuffled. The compressed videos generated from the same reference video are avoided from being presented consecutively. In the end, a user study is conducted after all the 13 sessions are accomplished, aiming at investigating the perceptibility of different distortion types in compressed face videos. The results is detailed in the supplementary. In total, 32 subjects participated in our study, from the age group of 22 to 30, and approximately half from each gender. All of them have fully participated in the whole process of this subjective quality test.

IV. DATA PROCESSING AND ANALYSES

A. Subjective Ratings Processing

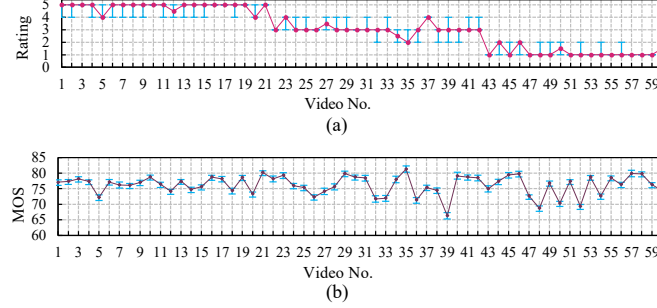


Fig. 7. The raw subjective ratings and obtained MOS values for each compressed video. (a) contains the subjective rating scores for 60 videos. The red dot denotes the median value among all subjects. The blue error bar denotes the first (25%) and third (75%) quartiles of subjective ratings. (b) contains the obtained MOS value of compressed videos. The dot in Tyrian purple denotes the MOS, and the blue error bar denotes the standard deviation. For the results of all compressed videos, please refer to the supplementary [76].

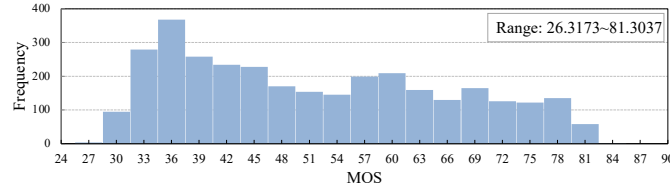


Fig. 8. Distribution of MOSs of compressed face videos in the proposed CFVQA benchmark.

The raw subjective rating data need to be screened before being mapped to the subjective quality score. Firstly, we examine the agreement of subjective ratings. Given one distorted video, it is generally believed that most subjects should reach agreements on the perceived quality. Herein, we employ quartiles of ratings to evaluate the subject agreement. As shown in Fig. 7, we show the first and third quartiles, corresponding to the median 50% of ratings in this range. Subsequently, we treat the videos with interquartile range (IQR) smaller than or equal to 1 as the videos with the agreement, implying that the opinions of the central 50% of subjects are constrained within an interval of one. We observe that 96.48% of the compressed face videos in the proposed database attain subjective agreement on the quality, which implies that the subjective testing on these videos could be robust and sustainable in building up the benchmark. Secondly, we screen subjective scores to identify unreliable participants following the procedures in [79] based on the 99% confidence interval of the subjective scores. Generally speaking, this procedure can particularly identify the subject with deviated ratings compared with most subjects. In this study, 2 out of 32 subjects have been rejected, and all scores of the rejected subjects are not included in further processing. Finally, the washed subjective ratings are converted into the Mean Opinion Scores (MOSs).

Initially, the Z-scores are given by,

$$Z_{ij} = \frac{S_{ij} - \mu_i}{\delta_i}, \quad (1)$$

where i and j denote subjective and test video indices. The μ_i and δ_i are the mean value and standard deviation on the quality rating S_{ij} of subject i . Subsequently, Z-scores are linearly mapped to the range of $[0, 100]$ under the assumption that Z-scores of one subject follow the standard Gaussian [81] in the range of $[-3, +3]$,

$$\tilde{Z}_{ij} = \frac{100(Z_{ij} + 3)}{6}. \quad (2)$$

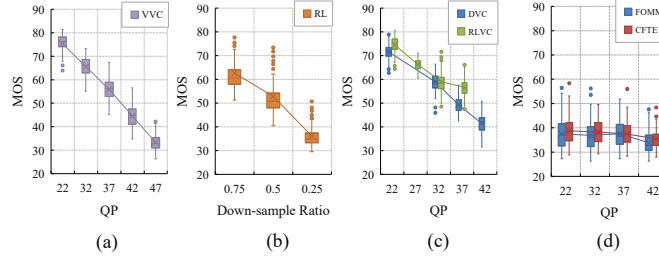


Fig. 9. Illustration of the MOS variations for different QPs. From bottom to top, the three horizontal lines of each box denote the lower quartile, median, and upper quartile of each subset, respectively. The boundary of the lower whisker is the minimum value, and the upper whisker boundary is the maximum value. The x notion denotes the mean value of each subset. All other observed data points outside the boundary of the whiskers are plotted as outliers. (a) Generative coding methods; (b) End-to-end coding methods; (c) VVC; (d) RL.

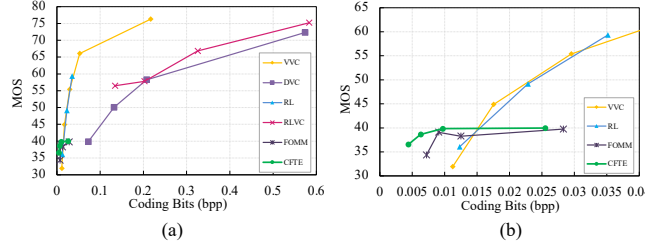


Fig. 10. The RD performance where the distortion is evaluated in terms of MOS. (a) The RD curve over the entire bit-rate range. (b) The RD curve in the low bit-rate range.

Finally, the MOS and corresponding standard deviation can be computed as

$$\omega_j = \frac{1}{N} \sum_{i=1}^N \tilde{Z}_{ij}, \quad (3)$$

$$\sigma_j = \sqrt{\frac{1}{N-1} \sum_{i=1}^N (\tilde{Z}_{ij} - \omega_j)^2}, \quad (4)$$

where N is the number of subjects involved. The distributions of the MOS values are illustrated in Fig. 8, from which it can be observed that the MOSs span from 26.3 to 81.3, covering a wide range of quality levels and substantially spanning the quality spectrum. Therefore, the proposed benchmark epitomizes reasonable perceptual quality separation identifiability.

B. Analyses of Subjective Quality

The MOS distributions for different QPs are shown in Fig. 9. Apparently, the MOSs drop with the increase of QP, though the variation sensitivity differs among these methods. This is not surprising as in FOMM and CFTE, the quality of the first frame controlled by QP is propagated to the subsequent frames by the generative models. As such, the distortions caused by generative models may play more dominant roles. Moreover, recall that the principle in generating compressed videos is ensuring the overlap in subjective quality. As shown in Fig. 9, there is a very apparent quality level overlap among different compression methods, though for generative compression methods the quality levels only span at the low range due to the unique low bit rate coding specialty.

In Fig. 10, the RD performance regarding the MOS values is illustrated. The bit rate and MOS values of a particular video coding codec are computed by the average values over the compressed videos generated from 32 randomly selected reference video sequences at a specific distortion level. The RD curve can reflect the coding performance faithfully when the quality is measured by the MOS. It can be observed that at the low bit rate range, the generative coding methods are significantly better than the other codecs, which has also been repeatedly observed in [14], [16]. Moreover, with the increase of the bit rate, the visual quality of the generative methods saturates because the distortions from generative models dominate the visual quality. It is also apparent that the performance of RL and VVC is also quite close, as both rely on VVC as the codec. In addition, E2E methods deliver high-quality compressed videos at the expense of a higher bit rate. However, it is worth mentioning that the goal of this work is not comparing different codecs but focusing on evaluating the distortions originating from these codecs instead.

TABLE III
PERFORMANCE OF THE MODELS ON THE PROPOSED DATABASE AND SUB-COLLECTIONS. LARGER PLCC, SRCC, AND KRCC VALUES WITH SMALLER RMSE VALUES INDICATE BETTER PERFORMANCE. IN EACH COLUMN, THE BEST PERFORMANCE OF EACH CATEGORY BOLD FACED. ASTERISK SUPERScript DENOTES THE PLCC IS COMPUTED AFTER DATA RESCALING.

Method	SRCC↑ for each subset						SRCC↑ for each subset			Overall			
	VVC	RL	DVC	RLVC	FOMM	CFTE	Traditional	End2end	Generative	PLCC↑	SRCC↑	KRCC↑	RMSE↓
PSNR	0.8997	0.8189	0.8147	0.6375	0.4636	0.4275	0.8794	0.7977	0.4112	0.9017	0.8749	0.6782	6.3026
SSIM	0.8400	0.7514	0.7416	0.5855	0.2980	0.2845	0.8153	0.7411	0.2669	0.8742	0.8477	0.6420	7.0766
MS-SSIM	0.9241	0.8230	0.8700	0.7400	0.5295	0.4808	0.8919	0.8636	0.4408	0.9152	0.8873	0.6975	5.8738
DISTS	0.9227	0.8861	0.8805	0.7864	0.5312	0.5542	0.9034	0.8751	0.5449	0.8377	0.8353	0.6420	14.5737
LPIPS	0.8836	0.7930	0.8108	0.7089	0.5218	0.5317	0.8552	0.8196	0.5008	0.8625	0.8644	0.6689	14.5737
MOVIE	0.9189	0.8787	0.8798	0.7904	0.2363	0.1051	0.9036	0.8753	0.1529	0.9199*	0.8766	0.6854	14.5737
STRRED	0.9499	0.7957	0.9233	0.7689	0.5477	0.6010	0.8653	0.8960	0.5628	0.9117	0.8902	0.7121	5.9862
VMAF	0.9476	0.9271	0.9046	0.7896	0.5472	0.4905	0.9443	0.8890	0.4737	0.9211	0.8984	0.7157	5.3166

V. PERFORMANCE OF OBJECTIVE QUALITY ASSESSMENT METHODS

To validate the performance of existing objective quality measures on the proposed database, eight main-stream non-blind image/video quality assessment methods are included to benchmark the objective quality of the CFVQA database. More specifically, five FR-IQA algorithms, including PSNR [82], SSIM [37], Multi-scale Structural Similarity (MS-SSIM) [38], DISTS [45], and LPIPS [44] are selected, among which DISTS and LPIPS are two data-driven algorithms based upon deep neural networks. Three popular non-blind VQA algorithms, including STRRED [56], VMAF [52] and MOVIE [49] are also involved. The performance is evaluated by Pearson Linear Correlation Coefficient (PLCC), Spearman Rank Correlation coefficient (SRCC), Kendall Rank Correlation Coefficient (KRCC), and Root-Mean-Square Error (RMSE). The objective quality scores are remapped by fitting the non-linear logistic regression function,

$$f(x) = \beta_1 \left(\frac{1}{2} - \frac{1}{1 + e^{\beta_2(x - \beta_3)}} \right) + \beta_4 x + \beta_5, \quad (5)$$

where β_1 to β_5 are the fitting parameters. As such, the PLCC and RMSE can be computed after non-linear fitting.

In Table III, the four criteria are evaluated on the entire database. The performance in terms of SRCC, which typically indicates the prediction monotonicity, is shown for each subset, including traditional methods (VVC and RL), E2E methods (DVC and RLVC), and generative methods (FOMM and CFTE). Note that the MOVIE scores are rescaled for easier linear regression. It is apparent that STRRED performs the best on four out of six compression subsets, except for RL and RLVC, on which the best performers are VMAF and MOVIE, respectively. For the quality assessment of videos compressed by the generative models, STRRED and the deep learning based model DISTS achieve the promising performance in terms of SRCC, but are still far from satisfactory. It can be explained by the fact that the GAN-based coding methods generate high-semantic-level distortions, like contour and shape, which HVS is more sensitive to. However, current objective measures focus overly on low-level statistical feature mismatches. It typically leads to overestimated quality degradation levels on the GAN-relative distortions, leading to lower correlations with MOSs. On the other side, MS-SSIM also delivers better performance when compared with SSIM either on the entire database scale or each video subset, revealing the superiority of the quality estimation in a multi-scale way.

Fig. 11 shows the scatter plots between the predicted quality of the utilized objective quality measurement and MOSs. These results exhibit that there are still major challenges in the effective quality evaluation of compressed face videos. It is not surprising to see that the videos from the traditional codec are relatively effortless to handle, while the performance of the E2E encoded videos is lower, potentially due to the flickering artifacts involved, implying that a more effective evaluation for temporal distortions is in need. Overall, the proposed dataset opens up new space for exploring more effective quality assessment models and sheds light on the design of future video compression algorithms.

VI. WHEN FACE PRIOR MEETS TEMPORAL PRIOR: A GENERALIZED VIDEO QUALITY ASSESSMENT MODEL FOR COMPRESSED FACE VIDEOS

To obtain the compressed video quality objectively, we propose a novel **FA**ce **VI**deo **O**bjective **I**nteger **R**ity index (named **FAVOR**). The designed philosophy meets both the face prior and temporal prior which all play important roles in human quality perception. Our model FAVOR which achieves promising performance on the proposed dataset and is free from any model retraining or fine-tuning, can serve as the alternative baseline in the development of future VQA measures and compression methods.

A. Framework

The flowchart of our FAVOR is presented in Fig. 12, which consists of two stages: (1) The *frame-level quality evaluation* with the face content prior. (2) The *quality aggregation* with the temporal memory prior. In particular, we first adopt a Siamese

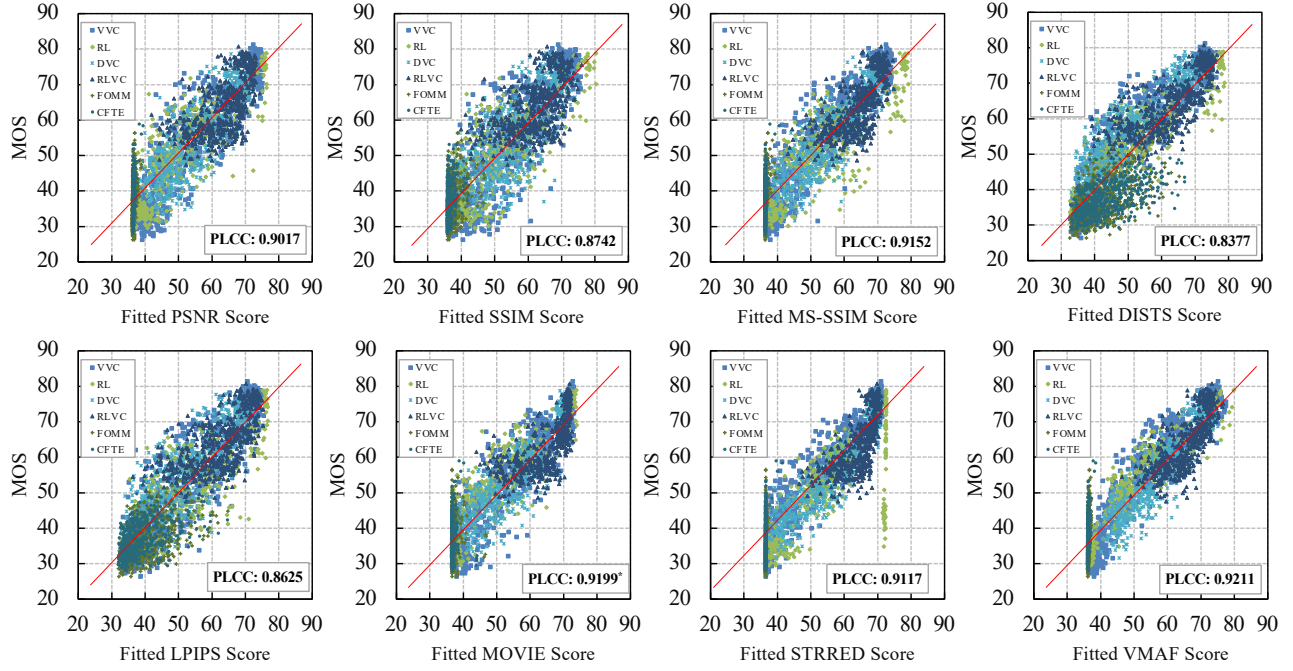


Fig. 11. Scatter plots of the objective quality scores and MOSs of all compressed face videos in the database. The more diagonally the data points are clustered, the better correlated between objective quality scores and MOSs.

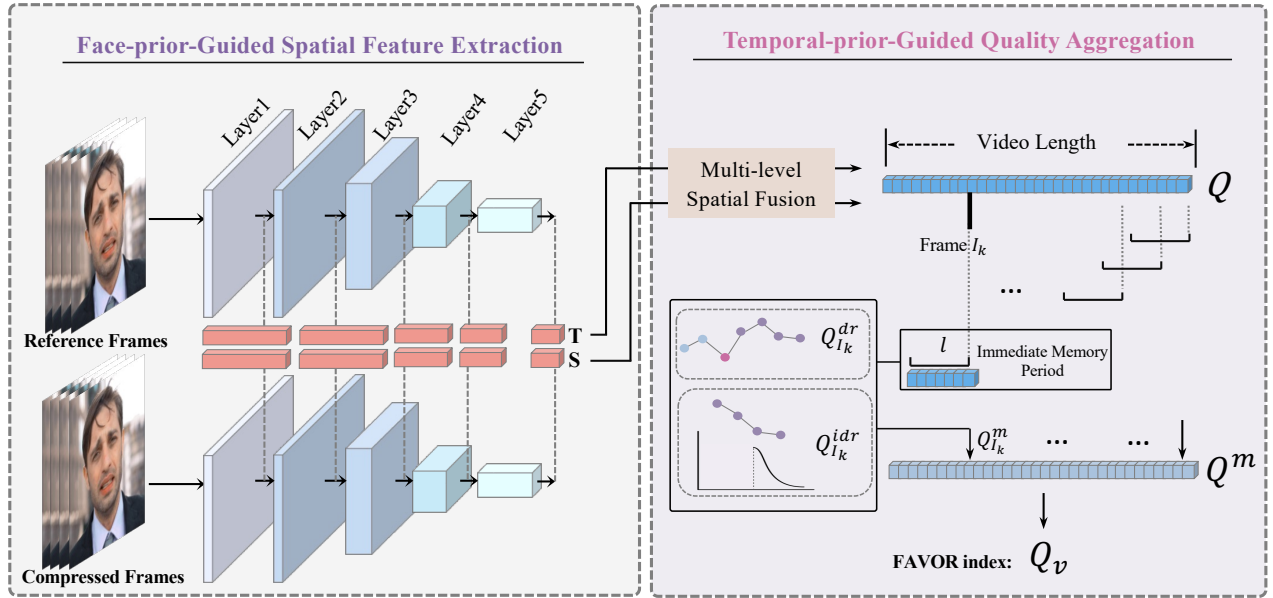


Fig. 12. The framework of the proposed FR-VQA method FAVOR. It contains the face-prior-guided spatial feature extraction module and the temporal-prior-guided quality fusion module which are sequentially connected.

network to extract quality-aware features for each frame in the reference and compressed face videos. The backbone of Siamese is a face recognition framework ResNet50 which has been fully trained on the MS-Celeb-1M (MS1M) database [83]. Herein, the backbone endows the extracted features with high relevance with HVS mechanism for face videos, which can be deemed as a strong spatial prior. Based upon the predicted frame-level quality, we further propose a human memory inspired quality aggregation module and finally achieve a promising prediction result for the whole video quality. The design details are elaborated as follows.

Frame-level Quality Prediction. To capture the quality of each frame, the similarity between the feature maps of the reference frame and distorted frame is evaluated. In particular, we adopt the statistics including the mean μ and standard deviation (std) δ of each feature map for the quality evaluation. As indicated in [45], the mean μ and std δ of the deep feature maps are highly correlated with image texture and structure, such that the quality can be effectively estimated by comparing the two

terms,

$$\begin{aligned} t_{i,j} &= \frac{2\mu_{i,j}^r \mu_{i,j}^d + \tau}{(\mu_{i,j}^r)^2 + (\mu_{i,j}^d)^2 + \tau}, \\ s_{i,j} &= \frac{2\delta_{i,j}^r \delta_{i,j}^d + \tau}{(\delta_{i,j}^r)^2 + (\delta_{i,j}^d)^2 + \tau}, \end{aligned} \quad (6)$$

where $t_{i,j}$ and $s_{i,j}$ denote the texture and structure similarity of the feature map of the j -th channel in the i -th stage. The $\mu_{i,j}^r$ and $\delta_{i,j}^r$ are the mean value and std value of the j -th channel in the i -th stage feature map of the reference frame, respectively. The $\mu_{i,j}^d$ and $\delta_{i,j}^d$ have the same meaning with $\mu_{i,j}^r$ and $\delta_{i,j}^r$, except they are extracted from the corresponding distorted frame. The $\delta_{i,j}^{rd}$ denotes the covariance between the reference and distorted features. The τ is a small positive offset to avoid zero division. Based upon Eqn. 6, for the k -th frame (denoted as I_k) of the test video, its frame-level quality (denoted as Q_{I_k}) can be derived by,

$$Q_{I_k} = \sum_{i=1}^M \sum_{j=1}^{N_i} (\alpha_{ij} t_{i,j} + \beta_{ij} s_{i,j}), \quad (7)$$

where α_{ij} and β_{ij} are two weights set defaultly as in [45]. M is the total layer number of the features extracted by the backbone and is set to 5, and N_i is the channel number of the i -th feature layer.

Frame-level Quality Aggregation. In this part, we aim to aggregate all the frame-level quality for the final video quality estimation. The aggregation philosophy is in line with the human memory effect during quality perception. The hysteresis is that the poor quality in the past frames would cause negative effects on current frame quality [84]. With such prior, we model the memory effect within the immediate memory period with the worst quality and refine it into two parts: the *direct effect* and the *indirect effect*. In detail, for the k -th frame I_k , its quality is refined by involving the two types of memory effects as follows,

$$Q_{I_k}^m = \begin{cases} Q_{I_k}, & k < l, \\ \gamma Q_{I_k}^{dr} + (1 - \gamma) Q_{I_k}^{idr}, & k \geq l. \end{cases} \quad (8)$$

The $Q_{I_k}^m$ is the refined quality and the $Q_{I_k}^{dr}$ and $Q_{I_k}^{idr}$ are the direct affected element and indirect affected element, by the past worst quality frame. The γ adjusts the levels of the two types of effects. In detail, as shown in Fig. 12, for frame I_k , we set the period of the immediate memory effect as the past l frames *aka* $\{I_{(k-l+1)}, I_{(k-l+2)}, \dots, I_k\}$. Suppose $k \geq l$, and the p -th frame in the interval is with the worst quality, *i.e.*, $Q_{I_{(k-l+p)}} = \min\{Q_{I_{(k-l+1)}}, Q_{I_{(k-l+2)}}, \dots, Q_{I_k}\}$, the direct effect element $Q_{I_k}^{dr}$ is defined by,

$$Q_{I_k}^{dr} = Q_{I_{(k-l+p)}}. \quad (9)$$

This element indicates the worst quality score of the past l frames plays a direct role in the current frame. In addition to the direct effect, the appearance of the worst frame also persuades the subject to pay much attention to its successive frames, which is deemed as the indirect effect of the worst-quality frame. We model the indirect effect as follows,

$$Q_{I_k}^{idr} = \sum_{z=1}^{l-p} w_z \cdot Q_{I_{(k-l+p+z)}}, \quad (10)$$

where w_z is the attention weight of the quality score of the z -th frame in the successive ones. In particular, $w_z = f(z^r)$ and $f(\cdot)$ is the descending half of Gaussian function where z^r is the quality rank of the z -th frame in the memory period (lower quality rank means lower quality score). The weighting philosophy lies in that the lower the quality, the negative effect is higher on the quality evaluation of frame I_k . Specifically, the w_s satisfy $\sum_{z=1}^{l-p} w_z = 1$. After refining the quality of each frame I_k with memory effect, the quality aggregation thus can be performed more reliably as follows,

$$Q_v = \frac{1}{L} \sum_{k=1}^L Q_{I_k}^m, \quad (11)$$

where the Q_v is the predicted quality of the compressed face video. L is the frame number of the video. Herein, a higher Q_v indicates a better video quality.

B. Performance Evaluations

Implementation Details. Our framework is implemented by PyTorch. We resize the video frame into a unified size of 112×112 . Five stages including 7-th, 16-th, 45-th, and the last convolutional layers of ResNet50 are adopt for feature comparison. The γ and l in the Eqn. 8 are set to 0.1 and 4 respectively.

Overall Performance. We compare the performance of the FAVOR index with other five IQA methods [37], [38], [44], [45], [82] and three VQA methods [49], [52], [56]. The IQA methods generate frame-level scores and are aggregated averagely to

TABLE IV
PERFORMANCE OF THE PROPOSED VQA METHOD ON THE CFVQA. THE BEST PERFORMANCE OF EACH CATEGORY IS HIGHLIGHTED IN BOLD.

Method	PLCC \uparrow	SRCC \uparrow	KRCC \uparrow	RMSE \downarrow
PSNR	0.9017	0.8749	0.6782	6.3026
SSIM	0.8742	0.8477	0.6420	7.0766
MS-SSIM	0.9152	0.8873	0.6975	5.8738
DISTS	0.8377	0.8353	0.6420	14.5737
LPIPS	0.8625	0.8644	0.6689	14.5737
MOVIE	0.9199*	0.8766	0.6854	14.5737
STRRED	0.9117	0.8902	0.7121	5.9862
VMAF	0.9211	0.8984	0.7157	5.3166
FAVOR	0.9229	0.9060	0.7248	5.6117

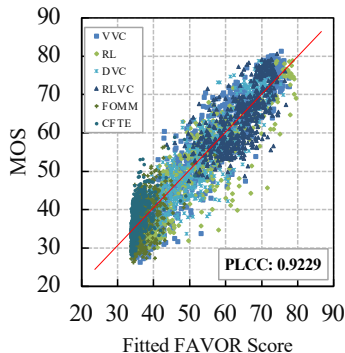


Fig. 13. Scatter plots of the proposed objective quality scores and MOSs of all compressed face videos in the database. The more diagonally the data points are clustered, the better correlated between objective quality scores and MOSs.

TABLE V
PERFORMANCE OF SPATIAL AND TEMPORAL MEASURES WHEN EVALUATED IN ISOLATION ON THE CFVQA DATABASE. 'T' DENOTES THE IQA METHODS AGGREGATED BY THE PROPOSED TEMPORAL AGGREGATION MODULE.

Method	PLCC \uparrow	SRCC \uparrow	KRCC \uparrow	RMSE \downarrow
average- Q_{I_k}	0.9068	0.8876	0.7123	5.7441
hysteresis- Q_{I_k}	0.9060	0.8997	0.7152	5.8462
recency- Q_{I_k}	0.9062	0.8857	0.6941	6.1619
VQPooling- Q_{I_k}	0.9001	0.8792	0.6887	6.5915
percentile- Q_{I_k}	0.9135	0.8915	0.7088	5.9281
primacy- Q_{I_k}	0.8307	0.7988	0.6111	8.1145
variation- Q_{I_k}	0.6330	0.6027	0.4327	11.2822
T-PSNR	0.9038	0.8803	0.6912	6.3011
T-SSIM	0.8900	0.8576	0.6513	6.8478
T-MS-SSIM	0.9158	0.8883	0.6980	5.8722
T-DISTS	0.8724	0.8572	0.6436	7.3779
T-LPIPS	0.8755	0.8689	0.6803	8.9137
FAVOR	0.9229	0.9060	0.7248	5.6117

compose the video quality score. The results are presented in Table IV and Fig. 11, which indicate that the proposed FAVOR index outperforms the other methods in terms of the PLCC, SRCC, and KRCC.

Ablation Study. The main components of our method are the face-prior-based quality predictor and the memory-prior-based quality aggregator. To reveal the effectiveness of each component, extensive ablation studies are conducted.

- *Study of the frame quality predictor.* In order to investigate the effectiveness of the quality predictor, we ablate it from our model and adopt other commonly-used IQA-based models for the frame-level quality prediction. The models compared against include PSNR, SSIM, MS-SSIM, DISTS, and LPIPS. The results of this study are presented in Table V, which reveals that all the alternatives lead to a performance drop. This observation indicates that more accurate quality can be obtained by incorporating facial prior information.
- *Study of the quality aggregator.* To study our memory-inspired aggregation strategy, we replace it with various aggregation modules, including the average pooling, temporal hysteresis [84], recency effect [85], percentile [86], primacy [85], and temporal variation [87]. The results are presented in Table V. It can be observed that our aggregation strategy outperforms the alternative strategies by a significant margin, demonstrating the high complementarity between our temporal quality aggregator and our spatial quality predictor. Moreover, from the Table, we can observe all the IQA-based models benefit

from our quality aggregator. For example, more than 0.02 SRCC performance gain can be achieved for DISTS when our aggregator is utilized. This phenomenon further proves the high-generalization capability of our quality aggregator.

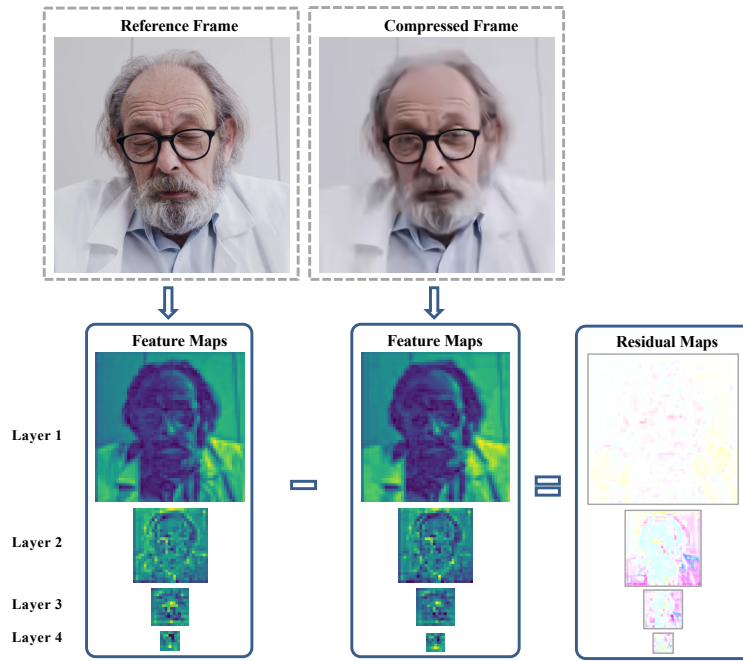


Fig. 14. Sampled feature maps from the four output layers of the ResNet decomposition of the reference frame and the VVC-compressed frame. Note the output of the fifth layer cannot be visualized due to it is a one-dimensional vector. More examples can be found in the supplementary.

Feature Visualisation. In Fig. 14, we present the feature maps of both the reference and corresponding compressed frame. The residual maps are further measured to visualize the quality corruption. From the residual maps, we can observe the quality degradation clues exist in different layers and the deeper the layer, the more detectable is the corruption. The reason may lie that the high-level semantics are severely corrupted after compression.

VII. CONCLUSIONS

In this paper, we have addressed a unique quality assessment problem that is critical for face video compression, coinciding with the accelerated development of artificial intelligence. We systematically study the problem by creating a dataset CFVQA and developing a dedicated FR-VQA algorithm named FAVOR. The dataset is featured with large scale (i.e., 103,680 labels with 3,240 distorted videos), multiple distortion types (i.e., traditional, E2E, and generative distortions), and a wide range of distortion levels. The objective VQA measure FAVOR, which particularly relies on spatial and temporal priors, has been validated to be effective without requiring any retraining process with the proposed dataset. This study, the first attempt at compressed face video quality assessment, has great potential to facilitate other compression or quality assessment research. For example, the visual quality assessment of semantic compression methods can be thoroughly investigated along this vein. Moreover, more advanced VQA methods that deliver robust performance over different distortion types can be developed for compressed videos.

REFERENCES

- [1] Y. Q. Zhang and S. Zafar, "Motion-compensated wavelet transform coding for color video compression," *IEEE Transactions on Circuits and Systems for Video Technology*, vol. 2, no. 3, pp. 285–296, 1992.
- [2] T. Wiegand, G. J. Sullivan, G. Bjontegaard, and A. Luthra, "Overview of the H. 264/AVC video coding standard," *IEEE Transactions on Circuits and Systems for Video Technology*, vol. 13, no. 7, pp. 560–576, 2003.
- [3] G. J. Sullivan, J. R. Ohm, W. J. Han, and T. Wiegand, "Overview of the High Efficiency Video Coding (HEVC) standard," *IEEE Transactions on Circuits and Systems for Video Technology*, vol. 22, no. 12, pp. 1649–1668, 2012.
- [4] B. Bross, Y.-K. Wang, Y. Ye, S. Liu, J. Chen, G. J. Sullivan, and J. R. Ohm, "Overview of the Versatile Video Coding (VVC) standard and its applications," *IEEE Transactions on Circuits and Systems for Video Technology*, vol. 31, no. 10, pp. 3736–3764, 2021.
- [5] G. Lu, W. Ouyang, D. Xu, X. Zhang, C. Cai, and Z. Gao, "DVC: An end-to-end deep video compression framework," in *Proceedings of the IEEE/CVF Conference on Computer Vision and Pattern Recognition*, 2019, pp. 11 006–11 015.
- [6] R. Yang, F. Mentzer, L. Van Gool, and R. Timofte, "Learning for video compression with recurrent auto-encoder and recurrent probability model," *IEEE Journal of Selected Topics in Signal Processing*, vol. 15, no. 2, pp. 388–401, 2020.
- [7] C. Jia, S. Wang, X. Zhang, S. Wang, J. Liu, S. Pu, and S. Ma, "Content-aware convolutional neural network for in-loop filtering in high efficiency video coding," *IEEE Transactions on Image Processing*, vol. 28, no. 7, pp. 3343–3356, 2019.
- [8] C. Ma, D. Liu, X. Peng, L. Li, and F. Wu, "Convolutional neural network-based arithmetic coding for HEVC intra-predicted residues," *IEEE Transactions on Circuits and Systems for Video Technology*, vol. 30, no. 7, pp. 1901–1916, 2019.

- [9] L. Zhu, S. Kwong, Y. Zhang, S. Wang, and X. Wang, "Generative adversarial network-based intra prediction for video coding," *IEEE Transactions on Multimedia*, vol. 22, no. 1, pp. 45–58, 2019.
- [10] Z. Hu, G. Lu, and D. Xu, "FVC: A new framework towards deep video compression in feature space," in *Proceedings of the IEEE/CVF Conference on Computer Vision and Pattern Recognition*, 2021, pp. 1502–1511.
- [11] R. Lopez and T. S. Huang, "Head pose computation for very low bit-rate video coding," in *International Conference on Computer Analysis of Images and Patterns*. Springer, 1995, pp. 440–447.
- [12] O. Wiles, A. Koepke, and A. Zisserman, "X2face: A network for controlling face generation using images, audio, and pose codes," in *Proceedings of the European Conference on Computer Vision*, 2018, pp. 670–686.
- [13] T. Wang, M. Liu, A. Tao, G. Liu, J. Kautz, and B. Catanzaro, "Few-shot video-to-video synthesis," *arXiv preprint arXiv:1910.12713*, 2019.
- [14] A. Siarohin, S. Lathuilière, S. Tulyakov, E. Ricci, and N. Sebe, "First order motion model for image animation," *Advances in Neural Information Processing Systems*, vol. 32, 2019.
- [15] M. Oquab, P. Stock, D. Haziza, T. Xu, P. Zhang, O. Celebi, Y. Hasson, P. Labatut, B. Bose Kolanu, T. Peyronel *et al.*, "Low bandwidth video-chat compression using deep generative models," in *Proceedings of the IEEE/CVF Conference on Computer Vision and Pattern Recognition*, 2021, pp. 2388–2397.
- [16] B. Chen, Z. Wang, B. Li, R. Lin, S. Wang, and Y. Ye, "Beyond keypoint coding: Temporal evolution inference with compact feature representation for talking face video compression," in *Data Compression Conference*. IEEE, 2022, pp. 13–22.
- [17] M. Nuutinen, T. Virtanen, M. Vaahteranoksa, T. Vuori, P. Oittinen, and J. Häkkinen, "CVD2014—A database for evaluating no-reference video quality assessment algorithms," *IEEE Transactions on Image Processing*, vol. 25, no. 7, pp. 3073–3086, 2016.
- [18] V. Hosu, F. Hahn, M. Jenadeleh, H. Lin, H. Men, T. Szirányi, S. Li, and D. Saupe, "The Konstanz natural video database (KoNViD-1k)," in *Ninth International Conference on Quality of Multimedia Experience*. IEEE, 2017, pp. 1–6.
- [19] D. Ghadiyaram, J. Pan, A. C. Bovik, A. K. Moorthy, P. Panda, and K. C. Yang, "In-capture mobile video distortions: A study of subjective behavior and objective algorithms," *IEEE Transactions on Circuits and Systems for Video Technology*, vol. 28, no. 9, pp. 2061–2077, 2017.
- [20] Z. Sinno and A. C. Bovik, "Large-scale study of perceptual video quality," *IEEE Transactions on Image Processing*, vol. 28, no. 2, pp. 612–627, 2018.
- [21] Y. Wang, S. Inguva, and B. Adsumilli, "Youtube UGC dataset for video compression research," in *21st International Workshop on Multimedia Signal Processing*. IEEE, 2019, pp. 1–5.
- [22] Z. Ying, M. Mandal, D. Ghadiyaram, and A. Bovik, "Patch-VQ: patching up the video quality problem," in *Proceedings of the IEEE/CVF Conference on Computer Vision and Pattern Recognition*, 2021, pp. 14 019–14 029.
- [23] F. De Simone, M. Naccari, M. Tagliasacchi, F. Dufaux, S. Tubaro, and T. Ebrahimi, "Subjective assessment of H. 264/AVC video sequences transmitted over a noisy channel," in *International Workshop on Quality of Multimedia Experience*. IEEE, 2009, pp. 204–209.
- [24] F. De Simone, M. Tagliasacchi, M. Naccari, S. Tubaro, and T. Ebrahimi, "A H. 264/AVC video database for the evaluation of quality metrics," in *2010 IEEE International Conference on Acoustics, Speech and Signal Processing*. IEEE, 2010, pp. 2430–2433.
- [25] A. K. Moorthy, L. K. Choi, A. C. Bovik, and G. De Veciana, "Video quality assessment on mobile devices: Subjective, behavioral and objective studies," *IEEE Journal of Selected Topics in Signal Processing*, vol. 6, no. 6, pp. 652–671, 2012.
- [26] K. Seshadrinathan, R. Soundararajan, A. C. Bovik, and L. K. Cormack, "Study of subjective and objective quality assessment of video," *IEEE Transactions on Image Processing*, vol. 19, no. 6, pp. 1427–1441, 2010.
- [27] F. Zhang, S. Li, L. Ma, Y. C. Wong, and K. N. Ngan, "IVP subjective quality video database," *The Chinese University of Hong Kong*, <http://ivp.ee.cuhk.edu.hk/research/database/subjective>, 2011.
- [28] Y. Pitrey, M. Barkowsky, R. Pépion, P. Le Callet, and H. Hlavacs, "Influence of the source content and encoding configuration on the perceived quality for scalable video coding," in *Human Vision and Electronic Imaging XVII*, vol. 8291. SPIE, 2012, pp. 460–467.
- [29] C. Keimel, A. Redl, and K. Diepold, "The TUM high definition video datasets," in *Fourth International Workshop on Quality of Multimedia Experience*. IEEE, 2012, pp. 97–102.
- [30] H. Wang, W. Gan, S. Hu, J. Y. Lin, L. Jin, L. Song, P. Wang, I. Katsavounidis, A. Aaron, and C.-C. J. Kuo, "MCL-JCV: a JND-based H. 264/AVC video quality assessment dataset," in *International Conference on Image Processing*. IEEE, 2016, pp. 1509–1513.
- [31] H. Wang, I. Katsavounidis, J. Zhou, J. Park, S. Lei, X. Zhou, M.-O. Pun, X. Jin, R. Wang, X. Wang *et al.*, "VideoSet: A large-scale compressed video quality dataset based on JND measurement," *Journal of Visual Communication and Image Representation*, vol. 46, pp. 292–302, 2017.
- [32] M. Cheon and J. S. Lee, "Subjective and objective quality assessment of compressed 4K UHD videos for immersive experience," *IEEE Transactions on Circuits and Systems for Video Technology*, vol. 28, no. 7, pp. 1467–1480, 2017.
- [33] C. G. Bampis, Z. Li, A. K. Moorthy, I. Katsavounidis, A. Aaron, and A. C. Bovik, "Study of temporal effects on subjective video quality of experience," *IEEE Transactions on Image Processing*, vol. 26, no. 11, pp. 5217–5231, 2017.
- [34] F. Zhang, F. M. Moss, R. Baddeley, and D. R. Bull, "BVI-HD: A video quality database for HEVC compressed and texture synthesized content," *IEEE Transactions on Multimedia*, vol. 20, no. 10, pp. 2620–2630, 2018.
- [35] M. Wang, J. Li, L. Zhang, K. Zhang, H. Liu, S. Wang, S. Kwong, and S. Ma, "Extended coding unit partitioning for future video coding," *IEEE Transactions on Image Processing*, vol. 29, pp. 2931–2946, 2019.
- [36] Y. Blau and T. Michaeli, "The perception-distortion tradeoff," in *Proceedings of the IEEE Conference on Computer Vision and Pattern Recognition*, 2018, pp. 6228–6237.
- [37] Z. Wang, A. C. Bovik, H. R. Sheikh, and E. P. Simoncelli, "Image quality assessment: from error visibility to structural similarity," *IEEE Transactions on Image Processing*, vol. 13, no. 4, pp. 600–612, 2004.
- [38] Z. Wang, E. P. Simoncelli, and A. C. Bovik, "Multiscale structural similarity for image quality assessment," in *Thirty-Seventh Asilomar Conference on Signals, Systems & Computers*, 2003, vol. 2. IEEE, 2003, pp. 1398–1402.
- [39] M. P. Sampat, Z. Wang, S. Gupta, A. C. Bovik, and M. K. Markey, "Complex wavelet structural similarity: A new image similarity index," *IEEE Transactions on Image Processing*, vol. 18, no. 11, pp. 2385–2401, 2009.
- [40] Z. Wang and Q. Li, "Information content weighting for perceptual image quality assessment," *IEEE Transactions on Image Processing*, vol. 20, no. 5, pp. 1185–1198, 2010.
- [41] L. Zhang, L. Zhang, X. Mou, and D. Zhang, "FSIM: A feature similarity index for image quality assessment," *IEEE Transactions on Image Processing*, vol. 20, no. 8, pp. 2378–2386, 2011.
- [42] A. Liu, W. Lin, and M. Narwaria, "Image quality assessment based on gradient similarity," *IEEE Transactions on Image Processing*, vol. 21, no. 4, pp. 1500–1512, 2011.
- [43] W. Xue, L. Zhang, X. Mou, and A. C. Bovik, "Gradient magnitude similarity deviation: A highly efficient perceptual image quality index," *IEEE Transactions on Image Processing*, vol. 23, no. 2, pp. 684–695, 2013.
- [44] R. Zhang, P. Isola, A. A. Efros, E. Shechtman, and O. Wang, "The unreasonable effectiveness of deep features as a perceptual metric," in *Proceedings of the IEEE/CVF Conference on Computer Vision and Pattern Recognition*, 2018, pp. 586–595.
- [45] K. Ding, K. Ma, S. Wang, and E. P. Simoncelli, "Image quality assessment: Unifying structure and texture similarity," *IEEE Transactions on Pattern Analysis and Machine Intelligence*, vol. 44, no. 5, pp. 2567–2581, 2020.
- [46] X. Liao, B. Chen, H. Zhu, S. Wang, M. Zhou, and S. Kwong, "DeepWSD: Projecting degradations in perceptual space to wasserstein distance in deep feature space," in *Proceedings of the 30th ACM International Conference on Multimedia*, 2022, pp. 970–978.
- [47] Y. Li, S. Wang, X. Zhang, S. Wang, S. Ma, and Y. Wang, "Quality assessment of end-to-end learned image compression: The benchmark and objective measure," in *Proceedings of the 29th ACM International Conference on Multimedia*, 2021, pp. 4297–4305.

- [48] K.-C. Yang, C. C. Guest, K. El-Maleh, and P. K. Das, "Perceptual temporal quality metric for compressed video," *IEEE Transactions on Multimedia*, vol. 9, no. 7, pp. 1528–1535, 2007.
- [49] K. Seshadrinathan and A. C. Bovik, "Motion tuned spatio-temporal quality assessment of natural videos," *IEEE Transactions on Image Processing*, vol. 19, no. 2, pp. 335–350, 2009.
- [50] A. K. Moorthy and A. C. Bovik, "Efficient video quality assessment along temporal trajectories," *IEEE Transactions on Circuits and Systems for Video Technology*, vol. 20, no. 11, pp. 1653–1658, 2010.
- [51] K. Manasa and S. S. Channappayya, "An optical flow-based full reference video quality assessment algorithm," *IEEE Transactions on Image Processing*, vol. 25, no. 6, pp. 2480–2492, 2016.
- [52] Z. Li, A. Aaron, I. Katsavounidis, A. Moorthy, and M. Manohara, "Toward a practical perceptual video quality metric," *The Netflix Tech Blog*, vol. 6, no. 2, p. 2, 2016.
- [53] C. G. Bampis, Z. Li, and A. C. Bovik, "Spatiotemporal feature integration and model fusion for full reference video quality assessment," *IEEE Transactions on Circuits and Systems for Video Technology*, vol. 29, no. 8, pp. 2256–2270, 2018.
- [54] W. Kim, J. Kim, S. Ahn, J. Kim, and S. Lee, "Deep video quality assessor: From spatio-temporal visual sensitivity to a convolutional neural aggregation network," in *Proceedings of the European Conference on Computer Vision*, 2018, pp. 219–234.
- [55] W. Kim, A.-D. Nguyen, S. Lee, and A. C. Bovik, "Dynamic receptive field generation for full-reference image quality assessment," *IEEE Transactions on Image Processing*, vol. 29, pp. 4219–4231, 2020.
- [56] R. Soundararajan and A. C. Bovik, "Video quality assessment by reduced reference spatio-temporal entropic differencing," *IEEE Transactions on Circuits and Systems for Video Technology*, vol. 23, no. 4, pp. 684–694, 2012.
- [57] L. Ma, S. Li, and K. N. Ngan, "Reduced-reference video quality assessment of compressed video sequences," *IEEE Transactions on Circuits and Systems for Video Technology*, vol. 22, no. 10, pp. 1441–1456, 2012.
- [58] X. Gao, S. Z. Li, R. Liu, and P. Zhang, "Standardization of face image sample quality," in *Advances in Biometrics: International Conference, Seoul, Korea, August 27-29, 2007. Proceedings*. Springer, 2007, pp. 242–251.
- [59] H. Sellahewa and S. A. Jassim, "Image-quality-based adaptive face recognition," *IEEE Transactions on Instrumentation and Measurement*, vol. 59, no. 4, pp. 805–813, 2010.
- [60] A. Abaza, M. A. Harrison, and T. Bourlai, "Quality metrics for practical face recognition," in *Proceedings of the 21st International Conference on Pattern Recognition*. IEEE, 2012, pp. 3103–3107.
- [61] P. Wasnik, K. B. Raja, R. Ramachandra, and C. Busch, "Assessing face image quality for smartphone based face recognition system," in *Fifth International Workshop on Biometrics and Forensics*. IEEE, 2017, pp. 1–6.
- [62] J. Yu, K. Sun, F. Gao, and S. Zhu, "Face biometric quality assessment via light CNN," *Pattern Recognition Letters*, vol. 107, pp. 25–32, 2018.
- [63] H.-I. Kim, S. H. Lee, and M. R. Yong, "Face image assessment learned with objective and relative face image qualities for improved face recognition," in *2015 IEEE International Conference on Image Processing*. IEEE, 2015, pp. 4027–4031.
- [64] G. Aggarwal, S. Biswas, P. J. Flynn, and K. W. Bowyer, "Predicting performance of face recognition systems: An image characterization approach," in *Workshops of Conference on Computer Vision and Pattern Recognition*. IEEE, 2011, pp. 52–59.
- [65] J. Hernandez-Ortega, J. Galbally, J. Fierrez, R. Haraksim, and L. Beslay, "Faceqnet: Quality assessment for face recognition based on deep learning," in *2019 International Conference on Biometrics*. IEEE, 2019, pp. 1–8.
- [66] P. Terhorst, J. N. Kolf, N. Damer, F. Kirchbuchner, and A. Kuijper, "SER-FIQ: Unsupervised estimation of face image quality based on stochastic embedding robustness," in *Proceedings of the IEEE/CVF Conference on Computer Vision and Pattern Recognition*, 2020, pp. 5651–5660.
- [67] F.-Z. Ou, X. Chen, R. Zhang, Y. Huang, S. Li, J. Li, Y. Li, L. Cao, and Y.-G. Wang, "SDD-FIQA: unsupervised face image quality assessment with similarity distribution distance," in *Proceedings of the IEEE/CVF Conference on Computer Vision and Pattern Recognition*, 2021, pp. 7670–7679.
- [68] L. Zhang, L. Zhang, and L. Li, "Illumination quality assessment for face images: A benchmark and a convolutional neural networks based model," in *Neural Information Processing: 24th International Conference, ICONIP 2017, Guangzhou, China, November 14-18, 2017, Proceedings, Part III 24*. Springer, 2017, pp. 583–593.
- [69] T. Schlett, C. Rathgeb, O. Henniger, J. Galbally, J. Fierrez, and C. Busch, "Face image quality assessment: A literature survey," *ACM Computing Surveys*, vol. 54, no. 10s, pp. 1–49, 2022.
- [70] S. Su, H. Lin, V. Hosu, O. Wiedemann, J. Sun, Y. Zhu, H. Liu, Y. Zhang, and D. Saupe, "Going the extra mile in face image quality assessment: A novel database and model," *arXiv preprint arXiv:2207.04904*, 2022.
- [71] B. Jo, D. Cho, I. K. Park, and S. Hong, "Ifqa: Interpretable face quality assessment," in *Proceedings of the IEEE/CVF Winter Conference on Applications of Computer Vision*, 2023, pp. 3444–3453.
- [72] "Pexels," [EB/OL], <https://www.pexels.com/videos/>, Accessed Oct 20, 2022.
- [73] "Mixkit," [EB/OL], <https://www.mixkit.com/videos/>, Accessed Oct 20, 2022.
- [74] F. M. Moss, K. Wang, F. Zhang, R. Baddeley, and D. R. Bull, "On the optimal presentation duration for subjective video quality assessment," *IEEE Transactions on Circuits and Systems for Video Technology*, vol. 26, no. 11, pp. 1977–1987, 2015.
- [75] F. M. Moss, C. T. Yeh, F. Zhang, R. Baddeley, and D. R. Bull, "Support for reduced presentation durations in subjective video quality assessment," *Signal Processing: Image Communication*, vol. 48, pp. 38–49, 2016.
- [76] "Compressed-face-videos-quality-assessment," [EB/OL], <https://github.com/Yixuan423/Compressed-Face-Videos-Quality-Assessment>, Accessed March 5, 2023.
- [77] K. Zeng, T. Zhao, A. Rehman, and Z. Wang, "Characterizing perceptual artifacts in compressed video streams," in *Human Vision and Electronic Imaging XIX*, vol. 9014. SPIE, 2014, pp. 173–182.
- [78] T. Installations and L. Line, "Subjective video quality assessment methods for multimedia applications," *Networks*, vol. 910, no. 37, p. 5, 1999.
- [79] R. I.-R. BT, "Methodology for the subjective assessment of the quality of television pictures," *International Telecommunication Union*, 2002.
- [80] "ARS by VQEG," [EB/OL], <http://www.its.bldrdoc.gov/vqeg/>, Accessed Oct 20, 2022.
- [81] K. Seshadrinathan, R. Soundararajan, A. C. Bovik, and L. K. Cormack, "Study of subjective and objective quality assessment of video," *IEEE Transactions on Image Processing*, vol. 19, no. 6, pp. 1427–1441, 2010.
- [82] Z. Wang and A. C. Bovik, "Mean squared error: Love it or leave it? a new look at signal fidelity measures," *IEEE Signal Processing Magazine*, vol. 26, no. 1, pp. 98–117, 2009.
- [83] J. Deng, J. Guo, N. Xue, and S. Zafeiriou, "Arcface: Additive angular margin loss for deep face recognition," in *Proceedings of the IEEE/CVF Conference on Computer Vision and Pattern Recognition*, 2019, pp. 4685–4694.
- [84] K. Seshadrinathan and A. C. Bovik, "Temporal hysteresis model of time varying subjective video quality," in *2011 IEEE International Conference on Acoustics, Speech and Signal Processing*. IEEE, 2011, pp. 1153–1156.
- [85] B. B. Murdock Jr, "The serial position effect of free recall," *Journal of Experimental Psychology*, vol. 64, no. 5, p. 482, 1962.
- [86] S. Rimac-Drlje, M. Vranjes, and D. Zagar, "Influence of temporal pooling method on the objective video quality evaluation," in *International Symposium on Broadband Multimedia Systems and Broadcasting*. IEEE, 2009, pp. 1–5.
- [87] A. Ninassi, O. Le Meur, P. Le Callet, and D. Barba, "Considering temporal variations of spatial visual distortions in video quality assessment," *IEEE Journal of Selected Topics in Signal Processing*, vol. 3, no. 2, pp. 253–265, 2009.